Quaternary Research

doi:10.1017/ qua.2019.10

Beryllium-10 dating of the Foothills Erratics Train in Alberta, Canada, indicates detachment of the Laurentide Ice Sheet from the Rocky Mountains at ~15 ka

Martin Margold[a,b]*, John C. Gosse[c], Alan J. Hidy[d], Robin J. Woywitka[a], Joseph M. Young[a], Duane Froese[a]

[a]Department of Earth and Atmospheric Sciences, University of Alberta, Edmonton, Alberta T6G 2E3, Canada
[b]Department of Physical Geography and Geoecology, Charles University in Prague, Faculty of Science, 128 43 Praha 2, Czech Republic
[c]Department of Earth Sciences, Dalhousie University, Halifax, Nova Scotia B3H 4R2, Canada
[d]Centre for Accelerator Mass Spectrometry, Lawrence Livermore National Laboratory, Livermore, California 94550, USA
*Corresponding author at: e-mail address: martin.margold@natur.cuni.cz (M. Margold).

(Received May 25, 2018; Accepted February 11, 2019)

Abstract

The Foothills Erratics Train consists of large quartzite blocks of Rocky Mountains origin deposited on the eastern slopes of the Rocky Mountain Foothills in Alberta between ~53.5°N and 49°N. The blocks were deposited in their present locations when the western margin of the Laurentide Ice Sheet (LIS) detached from the local ice masses of the Rocky Mountains, which initiated the opening of the southern end of the ice-free corridor between the Cordilleran Ice Sheet and the LIS. We use ^{10}Be exposure dating to constrain the beginning of this decoupling. Based on a group of 12 samples well-clustered in time, we date the detachment of the western LIS margin from the Rocky Mountain front to ~14.9 ± 0.9 ka. This is ~1000 years later than previously assumed, but a lack of a latitudinal trend in the ages over a distance of ~500 km is consistent with the rapid opening of a long wedge of unglaciated terrain portrayed in existing ice-retreat reconstructions. A later separation of the western LIS margin from the mountain front implies higher ice margin–retreat rates in order to meet the Younger Dryas ice margin position near the boundary of the Canadian Shield ~2000 years later.

Key words: Laurentide Ice Sheet; Cordilleran Ice Sheet; Rocky Mountains; ^{10}Be exposure dating; deglaciation

INTRODUCTION

The beginning of the last deglaciation in interior North America was marked by a separation of the Cordilleran and Laurentide Ice Sheets (CIS, LIS) and the formation of an ice-free corridor (IFC used through this paper) as the LIS retreated eastward from the eastern foot of the Rocky Mountains. The IFC has long been a subject of discussion because of its importance as a biogeographic connection between nonglaciated Beringia and the rest of the Americas south of the ice sheets (Johnston, 1933; Antevs, 1935; Mandryk et al., 2001; Goebel et al., 2008; Ives et al., 2014; Heintzman et al., 2016; Pedersen et al., 2016; Potter et al., 2017). Migration of animal species has been documented through the corridor (Shapiro et al., 2004; Heintzman et al., 2016) and, importantly, it has been suggested as one of the routes that humans might have taken when settling the Americas in the late Pleistocene (Johnston, 1933; Antevs, 1935; Haynes, 2002; Potter et al., 2017). Despite its importance for testing evolutionary models and the rates and nature of human migration in North America, relatively little information exists about the precise age of the initial opening of the IFC (Dyke et al., 2003; Dyke, 2004; Ives et al., 2014; Potter et al., 2017). The minimum limiting radiocarbon dates available are subject to a lag, of unknown duration, between the ice retreat and the deposition of the recovered organic material.

The IFC represents the land area formed as the LIS and CIS separated during deglaciation. The IFC measured more than 2000 km in length from north to south, and the last portion to open is suggested to have been between 62 and 65°N at 13–12.5 ^{14}C ka (15.6–14.8 cal ka; Dyke et al., 2003), in an area formerly occupied by the northern slopes of the Cordilleran–Laurentide ice saddle (Dyke and Prest, 1987; Tarasov et al., 2012; Peltier et al., 2015; Lambeck et al., 2017). However, the opening of the corridor started in the south, with a wedge of unglaciated terrain growing between the eastern front of the Rocky Mountains and the retreating

Cite this article: Margold, M., Gosse, J. C., Hidy, A. J., Woywitka, R. J., Young, J. M., Froese, D. 2019. Beryllium-10 dating of the Foothills Erratics Train in Alberta, Canada, indicates detachment of the Laurentide Ice Sheet from the Rocky Mountains at ~15 ka. *Quaternary Research* 1–14.

ice margin of the southwestern LIS (Dyke et al., 2003; Dyke, 2004). To establish a more precise age on the opening, it is desirable to use methods that directly date the initial ice retreat. Cosmogenic nuclide exposure dating of erratic boulders can provide such ages. Here we use ^{10}Be in quartz to determine the age of the Foothills Erratics Train (FET) in order to establish the timing of the separation of the southwestern LIS from the eastern front of the Rocky Mountains.

THE FOOTHILLS ERRATICS TRAIN

The FET consists of large quartzite blocks scattered in a linear pattern along the eastern foothills of the Rocky Mountains in southern Alberta. The FET stretches between ~53.5 and 49°N over a distance of almost 600 km (Stalker, 1956; Jackson et al., 1997; Jackson, 2017; Fig. 1), and its distribution documents the interaction between the local montane, Cordilleran, and Laurentide ice masses during the last glacial maximum (LGM; Fig. 1). The quartzite blocks of the FET originate from the Lower Cambrian Gog Group of the Canadian Rocky Mountains, likely largely but not exclusively, from the Mount Edith Cavell area of Jasper National Park (Mountjoy, 1958; Roed et al., 1967; Fig. 1). It has been speculated that the blocks were part of a rock fall from Mount Edith Cavell onto the surface of the Athabasca Valley glacier that brought them onto the foothills (Stalker, 1956; Jackson et al., 1997).

The highest portions of the Rocky Mountains hosted local ice-dispersal centres at the LGM, while at the regional scale, Cordilleran ice was drained from the Interior Plateau in British Columbia across the Continental Divide in the Rocky Mountains to the Interior Plains (Fig. 1). South of the Peace River, Cordilleran ice was deflected by Laurentide ice to flow in a southeasterly direction along the Rocky Mountain Foothills, forming a tributary of the High Plains Ice Stream, itself a branch of an ice-stream system draining the saddle between the CIS and the Keewatin Ice Dome of the LIS (Margold et al., 2018; Fig. 1). Local montane ice emanating from the eastern outlets of the Rocky Mountains was captured by this ice-stream system and flowed along the right lateral margin of the High Plains Ice Stream (Fig. 1). This configuration of ice masses is well documented by the dispersal pattern of the FET and the glacial geomorphological record of the Interior Plains (Ross et al., 2009; Margold et al., 2015, 2018).

The deposition of the FET marked the separation of the Laurentide and local montane ice masses and the initial deglaciation of the eastern slopes of the Rocky Mountains. A wedge of ice-free terrain formed between the Rocky Mountains and the Laurentide ice front retreating towards the northeast (White et al., 1985; Dyke and Prest, 1987; Dyke, 2004; Fig. 2).

The FET was a target of one of the early studies that employed cosmogenic nuclide exposure dating to reconstruct deglaciation ages. Jackson et al. (1997) dated eight samples from the FET by measuring whole-rock cosmogenic ^{36}Cl. The ages obtained ranged from 19.9 ± 2.5 to 10.8 ± 1.6 ka (excluding an outlier of 48.2 ± 6.5 ka; all ages are recalculated using an up-to-date production rate and scaling, and assume zero erosion; Fig. 2, Table 1, Supplementary Data) and they were, in combination with the study of Young et al. (1994), key to the argument that broad coalescence of the Laurentide, Cordilleran, and local montane ice masses in central and southern Alberta only happened in the Late Wisconsinan (Oxygen Isotope Stage 2). However, the relatively large spread of the ^{36}Cl ages prevented the authors from making inferences on the timing of the ice retreat. We have elected to resample some of the FET boulders dated by Jackson et al. (1997) along with others that were not previously dated. The ^{36}Cl chronometer has, in this case, two disadvantages. First, when whole-rock samples are used (as was common at the time of Jackson et al. [1997]), there is a variable but often significant component of ^{36}Cl that is produced when slow (thermal) cosmogenic or radiogenic neutrons are captured by native ^{35}Cl (the most abundant isotope of natural chlorine in rock minerals such as hornblende, biotite, and quartz fluid inclusions). The disadvantage therefore relates to the contribution to age uncertainty owing to (1) the difficulty of precisely measuring the ^{35}Cl concentration and (2) the inability to know the history of moisture contents and snow cover over millennial time scales, factors that moderate the thermal neutron flux in complex ways (Dunai et al., 2007; Zweck et al., 2013; Delunel et al., 2014). Second, the production rate of ^{36}Cl is more poorly defined than that of ^{10}Be (Phillips et al., 2016a, 2016b). We have therefore chosen to measure the ages using ^{10}Be, and we do so for 16 boulders that span the length of the FET.

METHODS

Samples for cosmogenic nuclide exposure dating were collected with a diamond-blade cutoff saw and a hammer and chisel. Samples ALT-MM-15-10 and ALT-MM-15-11 were collected with a hammer and chisel only to minimize the visible traces of the sampling on the erratic blocks in publicly sensitive areas. Because large erratic blocks can be objects of significance for the Canadian First Nations (Brink, 1981), we collaborated with the Alberta Archaeological Survey and inspected each sampled block closely to rule out the occurrence of artifacts or cultural modification.

The samples were prepared as BeO targets at CRISDal Lab, Dalhousie University, Halifax, Nova Scotia, Canada. To concentrate sufficient quartz (20 g) from each sample, the following procedure was used. The samples were cleaned, crushed, and ground, and the 250–355 mm fraction was rinsed, leached in aqua regia (2 hours), and etched in hydrofluoric (HF) before mineral separation using combinations of froth flotation, Frantz magnetic separation, air abrasion, heavy liquids, and controlled digestions of non-quartz phases using HF or hexafluorosilicic acids. When the quartz concentration was sufficiently pure (as determined optically and with <100 ppm Al and Ti as determined on a 1 g aliquot with the lab's Teledyne-Leeman Prodigy Inductively Coupled Plasma-Optical Emission Spectrometer), approximately 35 wt% of the dried quartz concentrate was removed in an ultrasonic bath with dilute HF as per Kohl and Nishiizumi (1992). The samples were spiked with approximately 240 µg Be of the lab's $BeCl_2$ carrier ('Be-Carrier-31-28Sept2012'; prepared from a deeply mined

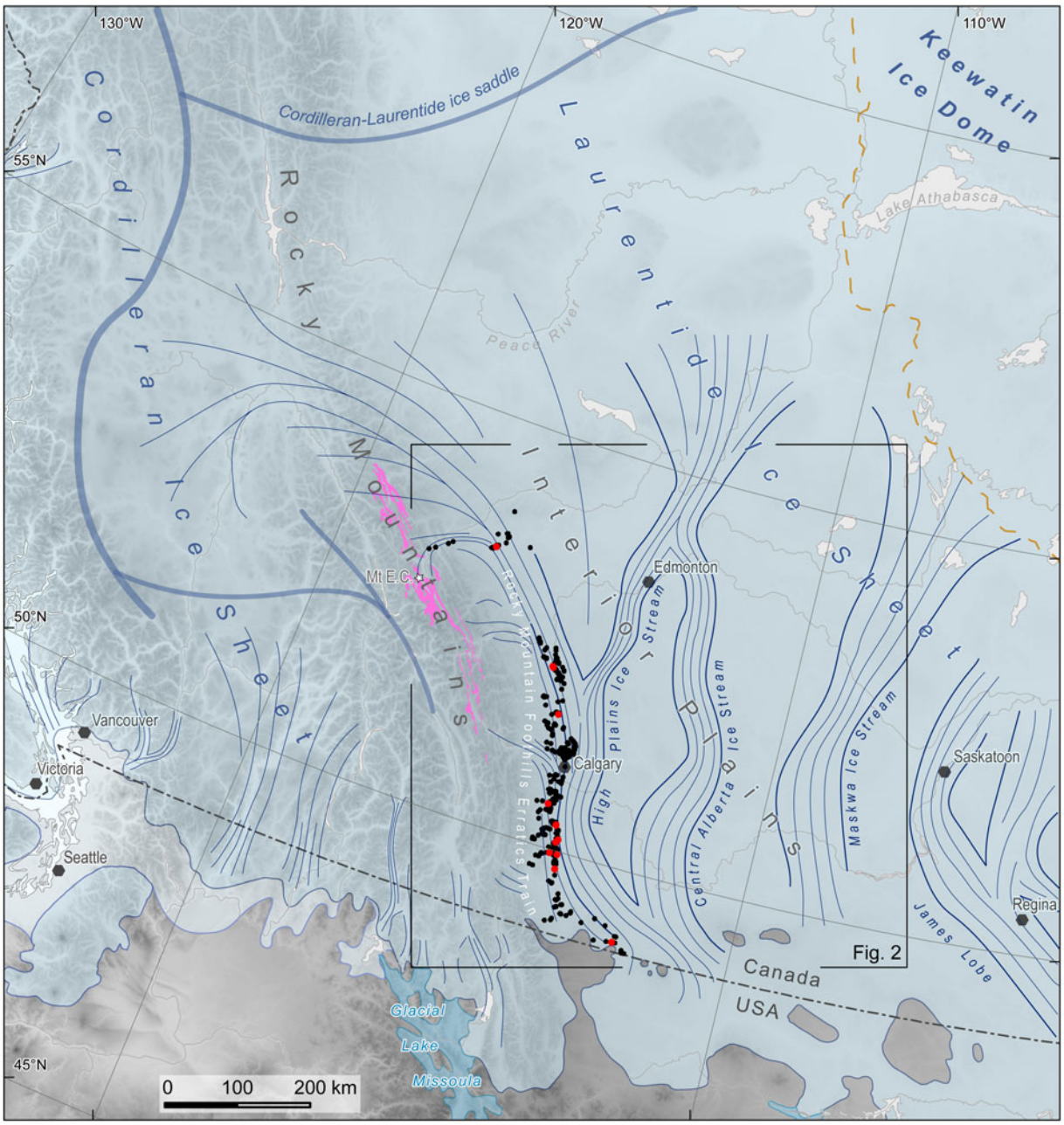

Figure 1. Regional ice sheet configuration at ~19 ka (16 ^{14}C ka) based on Dyke et al. (2003) and Margold et al. (2013, 2018) with time-transgressive maximum Wisconsinan/Fraser ice extent in lighter blue. Ice-flow direction is indicated by thin blue lines with lateral margins of major ice streams demarcated by bolder lines. Ice divides are drawn in blue-gray; note that the position of the ice divides in the Cordilleran Ice Sheet is little understood (cf. Margold et al., 2013; Seguinot et al., 2016). The Lower Cambrian Gog Group of the Canadian Rocky Mountains, the source of quartzite erratics, is drawn in pink, and the blocks of the FET mapped by Stalker (1956) are drawn in black. The localities of our samples are drawn in red. The location of Fig. 2 is indicated by a black rectangle. (For interpretation of the references to color in this figure legend, the reader is referred to the web version of this article.)

Ural Mountain phenacite with ^{10}Be/^{9}Be below 1×10^{-16}) and were digested in a HF-HNO_3 mixture, evaporated twice in perchloric acid, and treated with anion and cation column chemistry to isolate the Be^{2+}. After acidifying the samples with perchloric and nitric acid to remove residual B, $Be(OH)_2$ was precipitated using ultrapure ammonia gas, transferred to a cleaned boron-free quartz vial, and carefully calcined in a Bunsen burner flame to a white oxide for over 3 minutes. The BeO was powdered, mixed 2:3 by volume with high-purity niobium powder (325 mesh), and packed into stainless-steel cathodes for ^{10}Be/^{9}Be measurement at the Centre for Accelerator Mass Spectrometry, Lawrence Livermore National Lab, Livermore, California, USA. These measurements were made against the 07KNSTD3110 standard with a known ratio of ^{10}Be/^{9}Be = 2850×10^{-15} (Nishiizumi et al., 2007). Process blanks were also analyzed and used to subtract ^{10}Be introduced

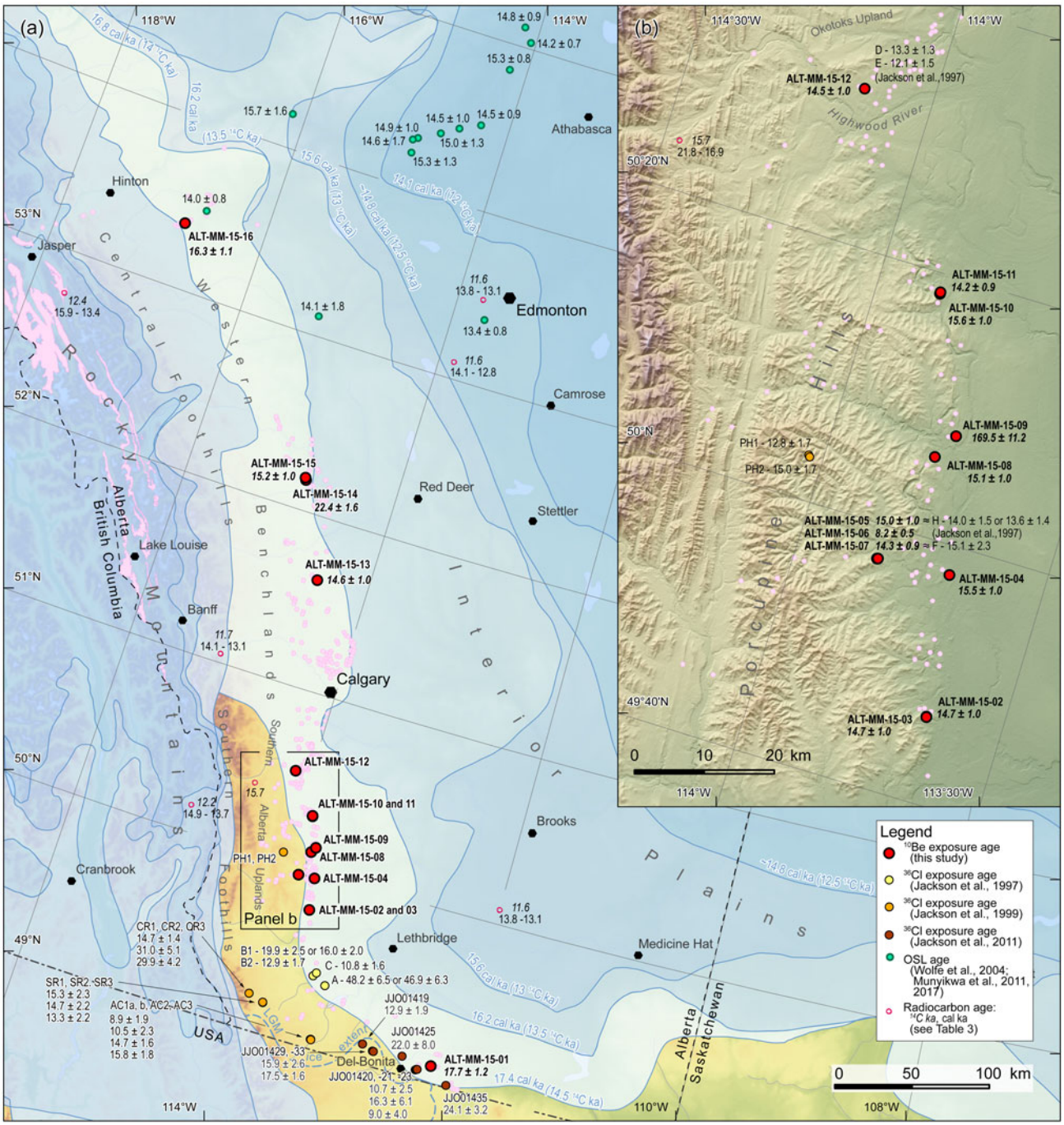

Figure 2. (a) Available chronological data in the region of the Foothills Erratics Train (FET). The Gog Group and the FET erratics are drawn in light pink. Available quantitative ages are drawn; see the legend for symbology, Table 1 for ^{36}Cl ages reported in Jackson et al. (1997, 1999, 2011), Table 2 for ages from this study, and Table 3 for available ^{14}C ages. Ice margin isochrones of Dyke et al. (2003) are drawn in shades of blue. (b) Close-up for the area of the Porcupine Hills. See panel a for location. (For interpretation of the references to color in this figure legend, the reader is referred to the web version of this article.)

during target preparation and analysis. For all samples, this correction was less than 1% of the adjusted ^{10}Be values.

Exposure ages were calculated using the online calculator by Balco et al. (2008; version 3.0, constants 3.0.3) and are reported here using the time-dependent CRONUS LSDn production rate scaling of Lal (1991) and Stone (2000), using the 'primary' calibration set of Borchers et al. (2016). Individual ages are reported with external error.

We report the exposure ages without a correction for snow shielding. The region has dry cold winters, resulting in a thin, low-density snowpack, and most of the sampled blocks were in the open and had substantial relief above the ground. It can thus be assumed that the top surfaces of the sampled blocks accumulate little to no snow in winter. Quartzite is a highly resistant lithology, and the surfaces of the sampled blocks were free of moss cover or other vegetation. Considering

Table 1. ^{36}Cl ages available for the region from the studies of Jackson et al. (1997, 1999, 2011).

Erratic block	Sample code	Latitude (°N)/longitude (°W)	Elevation (m above sea level)	Original reported age (zero erosion; ka)	Recalculated age[a] (zero erosion; ka)	Recalculated age[a] (2 mm/ka erosion; ka)
H (ALT-MM-15-05)	AE95102901[b]	49.9556/113.8361	1280	15.8 ± 0.4	14 ± 1.5	13.9 ± 1.6
H (ALT-MM-15-05)	AE95102901a[b]	49.9556/113.8361	1280	15.8 ± 0.4	13.6 ± 1.4	13.5 ± 1.5
B	AE95103103[b]	49.4147/113.4500	1076	17.6 ± 4.5	16 ± 2	15.4 ± 2.1
B	AE95103103a[b]	49.4147/113.4500	1076	17.6 ± 4.5	19.9 ± 2.5	19.1 ± 2.5
B	AE95103102[b]	49.4147/113.4500	1076	14.2 ± 4.3	12.9 ± 1.7	12.6 ± 1.6
F (ALT-MM-15-07)	AE95102903[b]	49.9567/113.8342	1235	17 ± 4	15.1 ± 2.3	14.4 ± 2.2
E (ALT-MM-15-12)	AE95103001[b]	50.5319/114.1383	1198	13.5 ± 0.5	12.1 ± 1.5	11.8 ± 1.7
D (ALT-MM-15-12)	AE95103002[b]	50.5319/114.1383	1198	14.2 ± 0.4	13.3 ± 1.3	13.3 ± 1.4
C	AE95103101[b]	49.4367/113.4272	1041	12 ± 0.6	10.8 ± 1.6	10.4 ± 1.4
A	AE95110101[b]	49.3811/113.3236	1082	53.3 ± 1.5	46.9 ± 6.3	43 ± 6
A	AE95110101a[b]	49.3811/113.3236	1082	53.3 ± 1.5	48.2 ± 6.5	44.6 ± 6.3
PH1	JJO96001[c]	50.0572/114.0286	1646	11.3 ± 8.9	12.8 ± 1.7	12.4 ± 1.5
PH2	JJO96002[c]	50.0553/114.0264	1646	13.7 ± 0.6	15 ± 1.7	14.8 ± 1.6
CR1	AE96101001[c]	49.2117/113.9489	1585	14.8 ± 0.7	14.7 ± 1.4	14.6 ± 1.4
CR2	AE96101003[c]	49.2117/113.9489	1585	15.5 ± 0.9	31 ± 5.1[e]	29.3 ± 4.6[e]
CR3	AE96101004[c]	49.2117/113.9489	1585	14.6 ± 0.8	29.9 ± 4.2[e]	29.8 ± 4.3[e]
SR1	JJO97001[c]	49.1836/113.8089	1325	18.3 ± 1.8	15.3 ± 2.3	14.6 ± 2.3
SR2	JJO97002[c]	49.1817/113.8089	1341	17.6 ± 0.8	14.7 ± 2.2	14.2 ± 2.1
SR3	JJO97003[c]	49.1817/113.8108	1341	15.4 ± 0.8	13.3 ± 2.2	12.6 ± 2.1
AC1a	JJO97004-1[c]	49.0558/113.3097	1448	11.7 ± 2.3	8.9 ± 1.9	8.4 ± 1.6
AC1b	JJO97004-2[c]	49.0558/113.3097	1448	13.3 ± 0.8	10.5 ± 2.3	10 ± 2
AC2	JJO97005[c]	49.0564/113.3106	1463	14.7 ± 0.8	14.7 ± 1.6	14.5 ± 1.7
AC3	JJO97006[c]	49.0544/113.3069	1418	16.7 ± 0.9	15.8 ± 1.8	15.5 ± 1.9
	JJO01419[d]	49.1153/112.8552	1273	13.5 ± 0.9	12.9 ± 1.9	12.3 ± 1.7
	JJO01420[d]	49.0542/112.3434	1197	11.5 ± 1.0	10.7 ± 2.5	10.2 ± 1.9
	JJO01421[d]	49.0576/112.3365	1204	18.9 ± 1.7	16.3 ± 6.1	14.7 ± 4.7
	JJO01423[d]	49.0598/112.3301	1208	10.9 ± 0.7	9 ± 4	8.8 ± 2.4
	JJO01425[d]	49.1107/112.4899	1196	25.7 ± 2.2	22 ± 8	19 ± 5
	JJO01429[d]	49.0911/112.7546	1250	18.2 ± 1.0	15.9 ± 2.6	15 ± 1.9
	JJO01433[d]	49.0910/112.7461	1273	19.3 ± 1.2	17.5 ± 1.6	17.5 ± 1.5
	JJO01435[d]	49.0145/112.0471	1059	28.3 ± 1.7	24.1 ± 3.2	22.4 ± 2.6

[a] See Supplementary Data for the methodology of the age recalculation.
[b] Jackson et al. (1997).
[c] Jackson et al. (1999).
[d] Jackson et al. (2011).
[e] Metadata indicated extremely high topographic shielding factors—possibly erroneous.

the aridity, hardness of the quartzite boulders, and a sampling strategy designed to target boulder surfaces with no evidence of erosion, we report the exposure ages without a correction for surface erosion. This is supported by the conclusions of Jackson et al. (1997, p. 197), who also suggested that erosion was negligible. However, because the erosion rates of our sampled surfaces remain unconstrained, we also provide a maximum age using the long-term quartzite bedrock erosion rates determined via ^{10}Be cosmogenic nuclides for the Shenandoah National Park, Virginia, USA (1.78 ± 0.2 mm ka^{-1}; Duxbury et al., 2015; Table 2).

FIELD SITES

Our data set stretches over the length of the FET in Canada (Figs. 1 and 2) between 49.1 and 53.8°N and is confined to elevations between 990 and 1230 m above sea level (m asl). The southernmost sample, ALT-MM-15-01, from the Del Bonita area (Figs. 2 and 3a), is of Shield origin (given its granite lithology) and thus does not belong to the FET, even though it is situated within the southeastern limit of the FET. Samples ALT-MM-15-02 to ALT-MM-15-11, all large quartzite blocks and thus members of the FET, were collected in the eastern slopes of the Porcupine Hills, a portion of the Southern Alberta Uplands that reaches up to ~1650 m asl (Fig. 2). Blocks from which samples ALT-MM-15-02 and ALT-MM-15-03 were taken were a part of a group of large quartzite blocks on a broad ledge at 1120 m asl, ~100 m above the foot of the slope where the Porcupine Hills rise from the plains (Figs. 2 and 3b and c). Sample ALT-MM-15-04 was collected from a block in the plain at 1006 m asl, 20 km N of ALT-MM-15-02 and ALT-MM-15-03 (Figs. 2 and 3d). Ten km to the west, samples ALT-MM-15-05 to ALT-MM-15-07 were collected from three large

Table 2. Cosmogenic ^{10}Be sample data and modeled surface exposure ages.

Sample code	Latitude (°N)/ longitude (°W)	Elevation (m above sea level)	Sample thickness[a] (cm)	Height of boulder above ground[b] (m)	Quartz[c] mass (g)	^{10}Be/^{9}Be[d] (× 10^{-15})	^{10}Be concentration[d] (× 10^{3} atoms/g SiO_2)	Age[d, e] zero erosion (ka)	Age[d, e] 2 mm/ka erosion (ka)
ALT-MM-15-01	49.10033/112.22257	1136	1.5	0.6	20.1252	237.9 ± 4.4	196.91 ± 5.33	17.7 ± 1.2	18.2 ± 1.2
ALT-MM-15-02	49.77851/113.65136	1122	1.5	2	20.1533	196.0 ± 3.8	163.58 ± 4.57	14.7 ± 1.0	15.1 ± 1.0
ALT-MM-15-03	49.77830/113.65108	1120	2.5	2	20.1697	195.3 ± 4.0	162.27 ± 4.66	14.7 ± 1.0	15.1 ± 1.0
ALT-MM-15-04	49.96253/113.68919	1006	1.5	3	20.5477	187.7 ± 3.7	157.42 ± 4.39	15.5 ± 1.0	15.9 ± 1.1
ALT-MM-15-05[f]	49.95547/113.83725	1231	1	3.3	15.2562	169.2 ± 3.1	183.40 ± 5.69	15.0 ± 1.0	15.4 ± 1.0
ALT-MM-15-06	49.95588/113.83614	1209	1.5	3.5	20.0417	120.3 ± 2.5	100.30 ± 2.88	8.2 ± 0.5	8.3 ± 0.6
ALT-MM-15-07[g]	49.95591/113.83578	1195	1	2.6	20.3954	207.2 ± 3.8	168.97 ± 4.57	14.3 ± 0.9	14.6 ± 1.0
ALT-MM-15-08	50.10248/113.78622	1132	2	1.6	15.2185	153.5 ± 3.7	165.04 ± 5.12	15.1 ± 1.0	15.5 ± 1.1
ALT-MM-15-09	50.13659/113.75736	1069	3.5	1.6	20.0722	2155.5 ± 22.2	1778.47 ± 40.00	169.5 ± 11.2	251.3 ± 26.6
ALT-MM-15-10	50.30623/113.87193	1177	1	2.2	20.4627	224.7 ± 4.2	183.34 ± 4.97	15.6 ± 1.0	16.0 ± 1.1
ALT-MM-15-11	50.30870/113.87212	1160	1	1.8	20.0275	197.9 ± 4.3	165.37 ± 4.91	14.2 ± 0.9	14.6 ± 1.0
ALT-MM-15-12[h]	50.53131/114.13990	1208	2	2.3	15.3571	159.2 ± 3.9	181.67 ± 5.64	14.5 ± 1.0	14.8 ± 1.0
ALT-MM-15-13	51.63497/114.47863	1150	4	1.2	15.2548	152.6 ± 3.2	164.88 ± 5.12	14.6 ± 1.0	14.9 ± 1.0
ALT-MM-15-14	52.17495/114.86999	1066	2	2	15.4246	228.6 ± 6.9	255.00 ± 7.91	22.4 ± 1.6	23.3 ± 1.7
ALT-MM-15-15	52.18727/114.88195	1069	2	3.2	15.4229	152.4 ± 4.3	164.42 ± 5.10	15.2 ± 1.0	15.6 ± 1.1
ALT-MM-15-16	53.38068/116.78810	991	2.5	1.2	15.0776	150.4 ± 3.8	159.97 ± 4.97	16.3 ± 1.1	16.7 ± 1.2

[a] The tops of all samples were exposed at the surface.
[b] Shielding factor is 1 for all samples.
[c] A density of 2.65 g/cm^3 was used based on the quartzite composition of the samples, with the exception of sample ALT-MM-15-01, for which a density of 2.7 g/cm^3 was used based on its granitic composition.
[d] All uncertainties are reported at the 1-sigma level. Blank corrected 10/9 ratios. See text for details on level of blanks.
[e] Exposure ages were calculated with the online calculator formerly known as CRONUS (Balco et al., 2008), version 3.0, constants 3.0.3 (http://hess.ess.washington.edu). Full details of the cosmogenic ^{10}Be analyses and exposure age calculations are provided in Methods Section.
[f] Jackson et al. (1997), sample H; see Fig. 2b, Table 1.
[g] Jackson et al. (1997), sample F; see Fig. 2b, Table 1.
[h] Jackson et al. (1997), samples D and E; see Fig. 2b, Table 1.

Table 3. Selected radiocarbon ages pertaining to the deglaciation of the southern Rocky Mountains and the western Interior Plains.[a]

Sample	Location		Elevation	Dated	Radiocarbon	Calibrated		
laboratory no.	Latitude (°N)	Longitude (°W)	(m asl)	material	(^{14}C yr BP)	(cal yr BP)	Locality	Reference
TO-2742	56.167	120.733	~ 600	Wood	13,970 ± 170	17,464–16,417	Ft. St John	Catto et al., 1996
AA-46352	56.28083	121.22750	~500	*Microtus*	12,567 ± 49	15,150–14,565	Bear Flat fan	Hebda et al., 2008
SFU-223	55.575	119.425	871	*Populus* wood	11,700 ± 260	14,223–13,030	Boone Lake	White et al., 1979, 1985; Bobrowski and Rutter, 1992
WAT-408	55.575	119.425	871	Gyttja	12,650 ± 320	15,991–13,946	Boone Lake	White et al., 1979
AECV-430C	52.75	117.66667	~1780	Lake sediments	12,350 ± 440	15,901–13,416	Lorraine Lake	Bobrowsky and Rutter, 1992
AECV-1203C	53.5	113.75	~710	*Bison*	11,620 ± 170	13,780–13,108	Clover Bar Pit	Burns, 1996
AECV-1117C	53.1	113.85	~815	Lake sediments[b]	11,570 ± 290	14,093–12,809	Wizard Lake	Beaudoin (unpublished), cited in Dyke et al., 2003
AECV-411C	54.517	110.5	550	Lake sediments	11,830 ± 330	14,896–13,063	Moore Lake	Hickman and Schweger, 1996
GSC-648	53.238	105.725	442	Lake sediments	11,560 ± 640	15,656–12,079	Prince Albert	Mott, 1973
S-246	50.83333	108.11667	~650	*Mammuthus*[c]	12,000 ± 200	14,645–13,432	Kyle	McCallum and Wittenberg, 1968
AECV-1053C	51.05	115.13333	~1500	Charcoal	11,680 ± 250	14,142–13,051	Bow Corridor	Newton (1991); Dyke et al., 2003
TO-5190	50.39583	114.46667	~1500	Wood in lake sediments[d]	15,670 ± 960	21,773–16,872	Cartwright L	Beierle and Smith, 1998
GSC-2275	50.15833	114.95555	1355	Wood	12,200 ± 160	14,897–13,731	Elkford	Harrison, 1976
OxA-14273	50.083	112	~780	*Equus conversidens*	11,620 ± 150	13,754–13,157	Gertzen site, Vauxhall	Burns, 2010

[a] The ages were calibrated using Oxcal 4.3 (Bronk Ramsey, 2009) with IntCal13 calibration curve (Reimer et al., 2013).
[b] Comments in Dyke et al. (2003): Possible hard-water error.
[c] Comments in Dyke et al. (2003): Questioned by Clayton et al. (1980) but not problematic for deglaciation; bone dates generally too young rather than too old.
[d] Comments in Dyke et al. (2003): Collector regards date as anomalously old for enclosing sediment; however, not improbable for this location (kettle lake).

Figure 3. (color online) Photographs of selected sampled blocks (see Fig. 2 for locations). (a) Sample ALT-MM-15-01 in the Del Bonita area. Note the chisel for scale. (b) A view in an eastern direction of the group of large blocks from which samples ALT-MM-15-02 and ALT-MM-15-03 were collected, with the Plains in the background. (c) Sample ALT-MM-15-02; see the person to the right of the block for scale. Sample ALT-MM-15-03 is visible in the background. (d) Sample ALT-MM-15-04. (e) View upslope of the group of large blocks from which samples ALT-MM-15-05 to ALT-MM-15-07 were collected. Sample ALT-MM-15-07 in the foreground (sample F of Jackson et al., 1997); note people for scale. Sample ALT-MM-15-05 is on the horizon (sample H of Jackson et al., 1997). (f) Sample ALT-MM-15-06, the young outlier. Note the split fragment on the right: the splitting could have affected the position of the rest of the block. (g) A view of the slope in which samples ALT-MM-15-05 to ALT-MM-15-07 are situated (their position is marked by white arrows). (h) Sample ALT-MM-15-08. (i) Sample ALT-MM-15-09, which returned an age of 169.5 ± 11.2 ka, a clear outlier. Concrete saw on the top of the block for scale. (j) Sample ALT-MM-15-12 (Jackson et al. [1997] sampled the two halves of the split block as their samples D and E). (k) Sample ALT-MM-15-14, which yielded an age of 22.4 ± 1.6 ka, an outlier. Person next to the block for scale. (l) Sample ALT-MM-15-16. Person next to the block for scale.

blocks perched on a slope of ∼15° (Figs. 2 and 3e–g). The relatively steep slope would normally render them unsuitable for cosmogenic nuclide exposure dating (owing to concerns about their postdeposition stability); however, they were sampled by Jackson et al. (1997; Fig. 2), returning ages close to the mean of their data set, and we thus resampled these blocks. Samples ALT-MM-15-08 and ALT-MM-15-09 were collected from blocks located on the opposite sides of a west–east-oriented valley mouth, several tens of metres above the plain to the east (Figs. 2 and 3h and i). The samples lie in between two generations of large ice-marginal meltwater channels oriented in a north–south direction (Jackson et al., 2008; Atkinson et al., 2014a; note that Rains et al. [2002] interpreted these channels as subglacial tunnel channels; Fig. 2b). Samples ALT-MM-15-10 and ALT-MM-15-11 were collected from a broad ledge in the eastern slope of the Porcupine Hills at a locality near the Nanton Erratic that is of cultural significance for its rock art (Fig. 2; Brink, 1981). The blocks we sampled were ∼100 m from the main erratic, and we inspected them closely to rule out the occurrence of cultural modification.

Sample ALT-MM-15-12 was collected from a block located in the broad valley of the Highwood River where it passes through the Okotoks Upland (Figs. 2 and 3j). The same block was sampled by Jackson et al. (1997; see Fig. 2b). The location of sample ALT-MM-15-13 was ∼120 km NNW of sample ALT-MM-15-12, in the Western Benchlands ∼20 km east of the foot of the Central Foothills (Fig. 2). Samples ALT-MM-15-14 and ALT-MM-15-15 were collected from two blocks at the transition from the plains into the Western Benchlands (Figs. 2 and 3k). North of here, the plains and the foothills become forested, and identification of erratics in the field becomes much more difficult than on the prairies. We only collected one more sample, ALT-MM-15-16, in an area east of Hinton (Figs. 2 and 3l).

With the exception of ALT-MM-15-01, all of the targeted blocks were large, with a height of 1.2 to 3.5 m above the ground. The sampled surfaces were devoid of weathering rinds, but some of the blocks have undergone splitting into several fragments. We attempted to avoid surfaces that could have originated from a fragmentation of the original block.

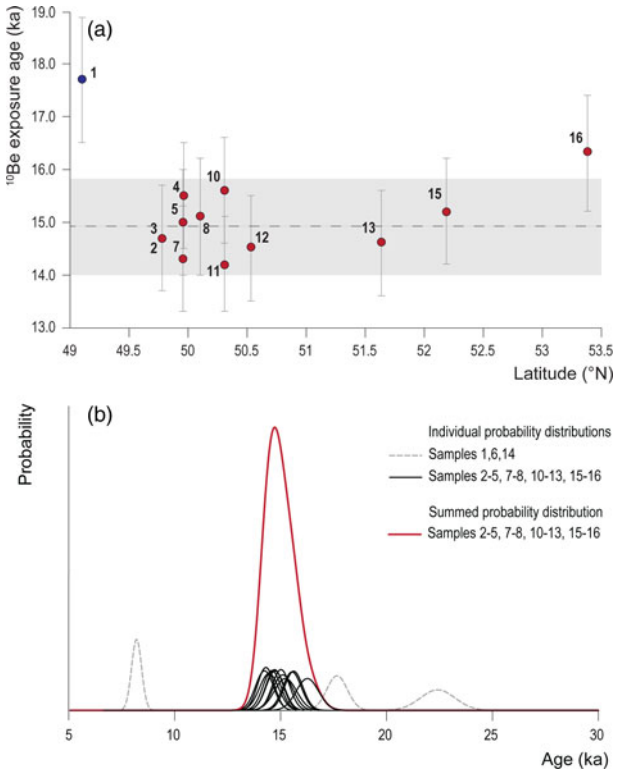

Figure 4. (Colour online) (a) Cosmogenic ^{10}Be apparent exposure ages plotted against the latitude at which the samples were collected. Note the lack of a clear trend (a decreasing age with increasing latitude would indicate a gradual unzipping of the Laurentide and local mountain ice masses). Outliers ALT-MM-15-06, ALT-MM-15-09, and ALT-MM-15-14 are not shown. The black horizontal line and the grey bar show the weighted mean age for the 12 displayed Foothills Erratics Train samples with its total ('external') uncertainty. (b) Probability distributions for the calculated ages (excluding the outliers ALT-MM-15-06, ALT-MM-15-09, and ALT-MM-15-14).

RESULTS

The ^{10}Be analytical data and exposure ages are presented in Table 2. Out of the 16 samples, three are clear outliers with ages that are incompatible with the regional glacial history: samples ALT-MM-15-09 and ALT-MM-15-14, which returned ages of 169.5 ± 11.2 and 22.4 ± 1.6 ka, respectively, and sample ALT-MM-15-06, which yielded an age of 8.2 ± 0.5 ka (the uncertainty stated for individual samples is their external error; i.e., uncertainty resulting from both the accelerator mass spectrometry (AMS) measurement and the adopted production rate). The remaining samples cluster between 17.7 ± 1.2 and 14.2 ± 0.9 ka (Figs. 2 and 4, Table 2). Even tighter clustering is reached when the only sample of Shield origin, ALT-MM-15-01 (17.7 ± 1.2 ka), is considered separately (Fig. 4). The remaining 12 samples fall into the period of ~2000 years between 16.3 ± 1.1 and 14.2 ± 0.9 ka. The weighted mean age of this group of 12 samples is 14.9 ka with a weighted standard deviation of 0.6 ka. This deviation is slightly larger than the mean internal uncertainty based solely on the AMS measurements (0.4 ka). Thus, to incorporate the more conservative internal error into the weighted mean age of the 12-sample data set, we combine in quadrature the weighted standard deviation (normalized by $\sqrt{n}$) with the mean systematic error (obtained by deconvolving the AMS-based internal errors from the total errors, which are output as external errors in the online calculator). The representative combined age for the FET data set is then 14.9 ± 0.2(0.9) ka (error format = internal (total or 'external')).

Within the individual sampling sites, the site where samples ALT-MM-15-02 and ALT-MM-15-03 were collected returned identical ages at three significant digits (Table 2). The remaining sites, where more than one sample was taken, display either a spread of ages above the weighted standard deviation of the 12-sample data set (15.0 ± 1.0 and 14.3 ± 0.9 ka, i.e., 0.7 ka for samples ALT-MM-15-05 and ALT-MM-15-07; and 15.6 ± 1.0 and 14.2 ± 0.9 ka, i.e., 1.4 ka for samples ALT-MM-15-10 and ALT-MM-15-11) or one of the ages is an outlier (Figs. 2 and 4).

All the collected samples are within a narrow elevation band, and therefore no correlation can be discerned between the measured age and elevation. Additionally, while the data set covers a considerable latitudinal distance (4.3° across the whole data set, 3.6° when only true FET samples are considered) and thus spans a significant stretch of the Laurentide–Cordilleran coalescence zone oriented in a NNW–SSE direction, no trends are observed between the deglaciation ages and latitude.

DISCUSSION

Interpreting ^{10}Be concentrations

The issues of incomplete exposure and nuclide inheritance affecting the measured ^{10}Be concentrations are commonly the main concerns when reconstructing deglaciation history with cosmogenic nuclide exposure dating (Heyman et al., 2011). However, in the case of the FET, the large size of the sampled blocks suggests that they have not emerged gradually from sediment matrix during the postdeposition period. The issue of incomplete exposure due to the degradation of landforms, on or within which the blocks were emplaced, can thus be ruled out. In contrast, nuclide inheritance most likely affected at least the oldest measured sample (ALT-MM-15-09; 169.5 ± 11.2 ka). We infer that the sampled surface was exposed in a cliff face for tens of thousands of years before its transport by ice and deposition at its current location. The age of the other old outlier (ALT-MM-15-14; 22.4 ± 1.6 ka) likely also results from nuclide inheritance, because the mid-LGM age cannot be a true deglaciation age, as all available records indicate that the region remained glaciated from about 25 ka (Young et al., 1994) until the late glacial (Jackson et al., 1997, 1999; Dyke et al., 2003; Dyke, 2004).

The only sample yielding an anomalously young age is ALT-MM-15-06, at 8.2 ± 0.5 ka. This is from a site where two other samples were measured at 15.0 ± 1.0 (ALT-MM-15-05) and 14.3 ± 0.9 ka (ALT-MM-15-07), and the measured age is thus a clear outlier. Samples ALT-MM-15-05 to

ALT-MM-15-07 were collected from the group of three large blocks targeted by Jackson et al. (1997; Fig. 3e–g), who report ages for their samples F (15.1 ± 2.3 ka) and H (14 ± 1.5) from that site (recalculated ages; Fig. 2, Table 1). The block sampled for ALT-MM-15-06, not sampled by Jackson et al. (1997), appeared to have split, and we assumed that the half we sampled was left in the original position (Fig. 3f). However, it is possible that the block turned during the splitting, and the sampled surface has thus only been in its present, unshielded position since then.

The remaining 13 ages fall within the post-LGM time. The oldest of these ages is the southernmost sample, ALT-MM-15-01, at 17.7 ± 1.2 ka, which is of Shield origin. The remaining 12 ages are well clustered, with the northernmost sample (ALT-MM-15-16) somewhat older that the remaining 11 samples south of it (Fig. 4), and we thus suggest that the age of deglaciation of the area in which the samples are located is within the time envelope they encompass (ca. 16.3 to 14.2 ka). These 12 samples stretch almost 500 km along the length of the foothills and, as noted, no trend is apparent in the ages with regard to the latitude of the samples (Fig. 4). Comparing the mean internal uncertainty (438 yr; including AMS measurement, carrier concentration uncertainty, and blank subtraction) with the weighted standard deviation (575 yr), we find the data scatter ~2.5% more than what would be expected from the internal uncertainties. This additional scatter may have several causes. First, nuclide inheritance may have been contributed when the rock was exposed in the mountains or during supraglacial transport (Stalker, 1956; Jackson et al., 1997). Even if the blocks only melted to the ice sheet surface in the later stages of their journey—they would have been rapidly covered by snow after falling onto the surface of the ice sheet in its accumulation area and would thus have been transported englacially for most of their journey (e.g., Dunning et al., 2015)—the blocks could still have seen centuries of exposure during their transport before being deposited at their current sites. This was noted by Jackson et al. (1997, p. 198), who stated that 'it is not known how long the erratics were situated on melting ice before they came to rest in their present positions. It is possible that they radically changed surface orientation or rolled one or more times over a period of hundreds or perhaps a thousand years before being let down on terra firma.'

Second, the glacial isostatic adjustment (GIA) of the landscape affects the measured nuclide concentrations; the weight of the continental ice sheets caused subsidence of the land surface, and our sampling sites were therefore at a lower elevation at the time when the FET blocks were emplaced and the sampled surfaces started accumulating ^{10}Be. However, most of the land surface rebound had already occurred during the thinning of the ice cover over the sampling sites and shortly after deglaciation, and the majority of the surface exposure history has therefore been at an elevation close to the modern (Lambeck et al., 2017). While some other studies employing the cosmogenic nuclide chronometer, especially those from the former ice dome areas (e.g., Ullman et al., 2016), apply a correction for the GIA based on the published GIA reconstructions, we chose not to do so. This is because: (1) most of our sampling sites were located relatively close to the southern margin of the LIS at the LGM and were thus likely only slightly affected by glacioisostasy; (2) the available GIA reconstructions display large differences for the region of the CIS–LIS ice saddle (cf. Peltier, 2004; Peltier et al., 2015; Lambeck et al., 2017), which broadens the uncertainty of the GIA correction; and (3) most of the GIA studies employ the ice sheet chronology of Dyke et al. (2003) in their reconstructions, while our aim is to produce independent deglaciation ages against which the existing ^{14}C chronology can be tested. The more northerly samples in our data set are more affected by the GIA than the southerly ones, and their real age is therefore somewhat older. This further weakens any age–latitude relationship (Fig. 4) and goes against the original hypothesis that the northerly samples should display younger ages, as would be expected for a gradual expansion of the IFC from the south.

Comparison of apparent ^{10}Be exposure ages from this study with other data on regional deglaciation

Available quantitative ages for the time of deglaciation of the eastern foot of the Rocky Mountains and the western part of the Interior Plains consist of radiocarbon, ^{36}Cl exposure dating, and optically stimulated luminescence (OSL) data. Radiocarbon dates on organic material provide minimum limiting ages on the timing of deglaciation. Consequently, only a few ^{14}C ages in western Alberta are older than 12 ^{14}C ka (14.1 cal ka; Table 3). OSL ages from dune fields along the Athabasca River north of Edmonton indicate deglaciation 1000 to 2000 years earlier compared with Dyke et al.'s (2003) ^{14}C-based ice-retreat reconstruction (Wolfe et al., 2004; Munyikwa et al., 2011, 2017; Fig. 2). Previous studies employing cosmogenic nuclide exposure dating in the Rocky Mountain Foothills and on the western Interior Plains have used ^{36}Cl (Jackson et al., 1997, 1999, 2011). The large spread of ^{36}Cl ages limits the interpretation of their spatial significance (Fig. 2, Table 1).

The age of our Shield sample (ALT-MM-15-01; Fig. 2, Table 2) at 17.7 ± 1.2 ka is consistent with the timing of ice retreat from the Del Bonita area reconstructed by Dyke et al. (2003), which they suggest occurred between 17.4 and 16.8 cal ka. To date the FET, we focus on a tightly clustered group of 12 ages between 16.3 ± 1.1 and 14.2 ± 0.9 ka, 8 of which are from the eastern slopes of the Porcupine Hills. We assume that the age of deglaciation is best approximated by the weighted mean age of the tightly clustered group of ages, which is 14.9 ± 0.9 ka. Our data thus indicate a later deglaciation of the southern foothills of the Rocky Mountains than suggested by Dyke et al. (2003). By ~14.8 ka (12.5 ^{14}C ka), Dyke et al. (2003) estimate the Laurentide ice front was ~200 km northeast from the foot of the Porcupine Hills (Fig. 2a), and they initiate the separation of the Laurentide and montane ice masses in the area of the Porcupine Hills already at ~19 ka to accommodate the 15.7 ^{14}C ka (21.8–16.9 cal ka) date of Beierle and Smith (1998; Fig. 2, Table 3).

Instead, the ^{10}Be data indicate the separation of the western Laurentide margin from the Rocky Mountain Foothills at ~15 ka. We dismiss the Beierle and Smith (1998) date as erroneous, in that it has never been reproduced and is in conflict with several lines of regional evidence (cf. Ives et al., 2014).

The separation of the local montane and south-flowing Cordilleran and Laurentide ice happened at about or before the onset of the Bølling warming (which started abruptly at 14.6 ka; Rasmussen et al., 2014) and possibly resulted from the gradual increase in the boreal summer insolation and the warming of climate over western North America after 16 ka, indicated by increasing water temperature in the Gulf of Alaska (Praetorius and Mix, 2014). It is also possible that the CIS, which reached its maximum extent at ~17 ka (Porter and Swanson, 1998; Margold et al., 2014; Stroeven et al., 2014) and likely had a dome over the Interior Plateau (Stumpf et al., 2000; Margold et al., 2013; Seguinot et al., 2016), blocked transport of precipitation farther east, decreasing precipitation over the CIS–LIS saddle and on the northwestern and southwestern slopes of the Keewatin Ice Dome (Dyke et al., 2002). By the time the ice masses separated, the LIS surface had already dropped considerably at the eastern Rocky Mountain front. The erratics we dated to ~15 ka are between 1000 and 1230 m asl, while the ice sheet surface had earlier covered the highest parts of the Porcupine Hills at >1600 m asl (Jackson et al., 1999). We do not distinguish any latitudinal trend in the separation of the Laurentide–Cordilleran and montane ice masses. A rapid opening of a long ice-free wedge along the southern Rocky Mountain front between 17 and 16 ka was suggested by Dyke et al. (2003). Based on the cosmogenic nuclide ages, the separation of the ice masses happened at least a millennium later than suggested by Dyke et al. (2003), but the spatial pattern of ice retreat they reported is supported by our results. The simultaneous detachment of the southwestern LIS margin from the mountain front might indicate a rapid weakening of the CIS–LIS saddle, and this inference is supported by the rapid succession of ice stream orientations on the Interior Plains (Margold et al., 2015, 2018).

Our ages indicate that the LIS margin retreated from the mountain front later than previously suggested, and if the Younger Dryas position of the LIS ice margin close to the boundary of the Canadian Shield in the ice margin chronology of Dyke et al. (2003) is correct, the ice-retreat rates over the Interior Plains must have been much higher than previously thought. The rapid ice retreat over the western Interior Plains coincided with the peak phase of the Bølling warming (Praetorius and Mix, 2014; Rasmussen et al., 2014, Menounos et al., 2017). Indeed, large ice-marginal meltwater channels in Alberta (Evans, 2000; Atkinson et al., 2014a, 2014b) bear witness to the significant meltwater produced during this period of rapid retreat.

Relations between FET and the IFC

The ages for the FET have a bearing on the initial opening of the IFC in western Canada. Our data indicate that the southern portion of the corridor, up to 53.5°N, opened at about 14.9 ± 0.2(0.9) ka. To trace the opening of the IFC farther north, more data are needed from the region that was located directly beneath the CIS–LIS saddle during the LGM and the early late glacial. Such data would help to constrain the IFC chronology, which has been a subject of a lively debate (Ives et al., 2014; Pedersen et al., 2016; Braje et al., 2017; Potter et al., 2017, 2018a, 2018b; Darvill et al., 2018) and for which a consensus has not yet been reached.

CONCLUSIONS

We applied ^{10}Be exposure dating to reduce the uncertainty in the age of the FET. The oldest sample in our data set after exclusion of outliers is the only sample of Shield origin, collected in the Del Bonita area, which dates to 17.6 ka. This age conforms well with the existing ice margin chronology of Dyke et al. (2003). We further focus on the well-clustered group of 12 samples, 8 of which are from the Porcupine Hills, for our inferences on the regional deglaciation history. The weighted mean age of the well-clustered group is 14.9 ± 0.9 ka. This overlaps with the onset of the Bølling warming, but the ice sheet surface must have already dropped considerably, as it had earlier covered the summit areas of the Porcupine Hills. Our results indicate that the detachment of the south-flowing Cordilleran and Laurentide ice from the local ice masses emanating from the Rocky Mountains occurred at least 1 ka later than previously reported. However, the lack of a latitudinal trend in the obtained ages is consistent with the rapid opening of an IFC reconstructed in the ice margin chronology of Dyke et al. (2003). A later separation of the LIS ice margin from the mountain front implies higher ice margin–retreat rates on the Interior Plains in order to meet the Younger Dryas ice margin position near the boundary of the Canadian Shield. To trace the separation of the Laurentide and Cordilleran ice masses farther north and to better constrain the timing of the final opening of the IFC as a passable route from north to south or vice versa, more data are needed from the region that was located directly underneath the CIS–LIS ice saddle during the LGM and the early late glacial.

SUPPLEMENTARY MATERIAL

The supplementary material for this article can be found at https://doi.org/10.1017/qua.2019.10.

ACKNOWLEDGMENTS

MM was supported by International Postdoctoral Fellowship no. 637-2014-483 from the Swedish Research Council. DF and JCG acknowledge funding from Natural Science and Engineering Research Council Discovery grants, and DF acknowledges funding from the Canada Research Chairs program. We thank Fred Phillips for providing data for the published ^{36}Cl ages and Richard Jones for discussing the effects of GIA on our samples. We are grateful for the mineral separation and BeO target chemistry by G. Yang and J. McKenna at Dalhousie University. This work was performed in part under the auspices of the U.S. Department of Energy by Lawrence Livermore National Laboratory under Contract

DE-AC52- 07NA27344. This is LLNL-JRNL-735369. We thank the associate editor Tom Lowell and two anonymous reviewers for their insightful comments, which helped us to improve the article.

REFERENCES

Antevs, E., 1935. The spread of aboriginal man to North America. *Geographical Review* 25, 302–309.

Atkinson, N., Utting, D.J., Pawley, S.M., 2014a. Glacial Landforms of Alberta. AER/AGS Map 604. Alberta Energy Regulator, Edmonton.

Atkinson, N., Utting, D.J., Pawley, S.M., 2014b. Landform signature of the Laurentide and Cordilleran ice sheets across Alberta during the last glaciation. *Canadian Journal of Earth Sciences* 51, 1067–1083.

Balco, G., Stone, J.O., Lifton, N.A., Dunai, T.J., 2008. A complete and easily accessible means of calculating surface exposure ages or erosion rates from ^{10}Be and ^{26}Al measurements. *Quaternary Geochronology* 3, 174–195.

Beierle, B., Smith, D.G., 1998. Severe drought in the early Holocene (10,000–6800 BP) interpreted from lake sediment cores, southwestern Alberta, Canada. *Palaeogeography, Palaeoclimatology, Palaeoecology* 140, 75–83.

Bobrowsky, P., Rutter, N., 1992. The quaternary geologic history of the Canadian Rocky Mountains. *Géographie physique et Quaternaire* 46, 5–50.

Borchers, B., Marrero, S., Balco, G., Caffee, M., Goehring, B., Lifton, N., Nishiizumi, K., Phillips, F., Schaefer, J., Stone, J., 2016. Geological calibration of spallation production rates in the CRONUS-Earth project. *Quaternary Geochronology* 31, 188–198.

Braje, T.J., Dillehay, T.D., Erlandson, J.M., Klein, R.G., Rick, T.C., 2017. Finding the first Americans. *Science* 358, 592–594.

Brink, J., 1981. Rock art sites in Alberta: retrospect and prospect. In: Moore, T.A. (Ed.), *Alberta Archaeology: Prospect and Retrospect*. Archaeological Society of Alberta, Lethbridge, pp. 69–82.

Bronk Ramsey, C., 2009. Bayesian analysis of radiocarbon dates. *Radiocarbon* 51, 337–360.

Burns, J.A., 1996. Vertebrate paleontology and the alleged ice-free corridor: the meat of the matter. *Quaternary International* 32, 107–112.

Burns, J.A., 2010. Mammalian faunal dynamics in late Pleistocene Alberta, Canada. *Quaternary International* 217, 37–42.

Catto, N., Liverman, D.G.E., Bobrowsky, P.T., Rutter, N., 1996. Laurentide, Cordilleran, and montane glaciation in the western Peace River—Grande Prairie region, Alberta and British Columbia, Canada. *Quaternary International* 32, 21–32.

Clayton, L., Moran, S.R., Bluemle, J.P., 1980. *Explanatory Text to Accompany the Geologic Map of North Dakota*. North Dakota Geological Survey Report of Investigation 69, 93 pp.

Darvill, C.M., Menounos, B., Goehring, B.M., Lian, O.B., Caffee, M.W., 2018. Retreat of the western Cordilleran Ice Sheet margin during the last deglaciation. *Geophysical Research Letters* 45, 9710–9720.

Delunel, R., Bourles, D.L., van der Beek, P.A., Schlunegger, F., Leya, I., Masarik, J., Paquet, E., 2014. Snow shielding factors for cosmogenic nuclide dating inferred from long-term neutron detector monitoring. *Quaternary Geochronology* 24, 16–26.

Dunai, T.J., Stuart, F.M., Pik, R., Burnard, P., Gayer, E., 2007. Production of ^{3}He in crustal rocks by cosmogenic thermal neutrons. *Earth and Planetary Science Letters* 258, 228–236.

Dunning, S.A., Rosser, N.J., McColl, S.T., Reznichenko, N.V., 2015. Rapid sequestration of rock avalanche deposits within glaciers. *Nature Communications* 6, 7964.

Duxbury, J., Bierman, P.R., Portenga, E.W., Pavich, M.J., Southworth, S., Freeman, S.P., 2015. Erosion rates in and around Shenandoah National Park, Virginia, determined using analysis of cosmogenic ^{10}Be. *American Journal of Science* 315, 46–76.

Dyke, A.S., 2004. An outline of North American deglaciation with emphasis on central and northern Canada. In: Ehlers, J., Gibbard, P.L. (Eds.), *Quaternary Glaciations—Extent and Chronology*. Part II. Elsevier, Amsterdam, pp. 373–424.

Dyke, A.S., Andrews, J.T., Clark, P.U., England, J.H., Miller, G.H., Shaw, J., Veillette, J.J., 2002. The Laurentide and Innuitian ice sheets during the Last Glacial Maximum. *Quaternary Science Reviews* 21, 9–31.

Dyke, A.S., Moore, A., Robertson, L., 2003. *Deglaciation of North America*. Geological Survey of Canada, Ottawa.

Dyke, A.S., Prest, V.K., 1987. Late Wisconsinan and Holocene history of the Laurentide ice sheet. *Géographie physique et Quaternaire* 41, 237–263.

Evans, D.J.A., 2000. Quaternary geology and geomorphology of the Dinosaur Provincial Park area and surrounding plains, Alberta, Canada: the identification of former glacial lobes, drainage diversions and meltwater flood tracks. *Quaternary Science Reviews* 19, 931–958.

Goebel, T., Waters, M.R., O'Rourke, D.H., 2008. The late Pleistocene dispersal of modern humans in the Americas. *Science* 319, 1497–1502.

Harrison, J.E., 1976. Dated organic material below Mazama (?) tephra: Elk Valley, British Columbia. In: Blackadar, R.G., Griffin, P.J., Dumych, H., Irish, W.J.W. (Eds.), *Report of Activities*. Part C. Geological Survey of Canada, Ottawa, pp. 169–170.

Haynes, G., 2002. *The Early Settlement of North America: The Clovis Era*. Cambridge University Press, Cambridge.

Hebda, R.J., Burns, J.A., Geertsema, M., Jull, A.J.T., 2008. AMS-dated late Pleistocene taiga vole (Rodentia: *Microtus xanthognathus*) from northeast British Columbia, Canada: a cautionary lesson in chronology. *Canadian Journal of Earth Sciences* 45, 611–618.

Heintzman, P.D., Froese, D., Ives, J.W., Soares, A.E.R., Zazula, G.D., Letts, B., Andrews, T.D., *et al*., 2016. Bison phylogeography constrains dispersal and viability of the Ice Free Corridor in western Canada. *Proceedings of the National Academy of Sciences USA* 113, 8057–8063.

Heyman, J., Stroeven, A.P., Harbor, J.M., Caffee, M.W., 2011. Too young or too old: evaluating cosmogenic exposure dating based on an analysis of compiled boulder exposure ages. *Earth and Planetary Science Letters* 302, 71–80.

Hickman, M., Schweger, C.E., 1996. The Late Quaternary palaeoenvironmental history of a presently deep freshwater lake in east-central Alberta, Canada and palaeoclimate implications. *Palaeogeography, Palaeoclimatology, Palaeoecology* 123, 161–178.

Ives, J.W., Froese, D., Supernant, K., Yanicki, G., 2014. Vectors, vestiges and Valhallas: rethinking the corridor. In: Graf, K.E., Ketron, C.V., Waters, M.R. (Eds.), *Paleoamerican Odyssey*. Texas A&M University Press, College Station, pp. 149–169.

Jackson, L.E., 2017. The Foothills Erratics Train region. In: Slaymaker, O. (Ed.), *Landscapes and Landforms of Western Canada*. Springer International Publishing, Cham, pp. 157–165.

Jackson, L.E., Andriashek, L.D., Phillips, F.M., 2011. Limits of successive middle and late Pleistocene continental ice sheets, Interior Plains of southern and central Alberta and adjacent areas. In: Ehlers, J., Gibbard, P.L., Hughes, P.D. (Eds.),

Quaternary Glaciations—Extent and Chronology: A Closer Look. Elsevier, Amsterdam, pp. 575–589.

Jackson, L.E., Phillips, F.M., Little, E.C., 1999. Cosmogenic ^{36}Cl dating of the maximum limit of the Laurentide Ice Sheet in southwestern Alberta. *Canadian Journal of Earth Sciences* 36, 1347–1356.

Jackson, L.E., Phillips, F.M., Shimamura, K., Little, E.C., 1997. Cosmogenic ^{36}Cl dating of the Foothills erratics train, Alberta, Canada. *Geology* 25, 195–198.

Jackson, L.E., Jr., Leboe, E.R., Little, E.C., Holme, P.J., Hicock, S.R., Shimamura, K., Nelson, F.E.N., 2008. *Quaternary Stratigraphy and Geology of the Rocky Mountain Foothills, Southwestern Alberta*. Geological Survey of Canada Bulletin 583. Natural Resources Canada, Ottawa.

Johnston, W., 1933. Quaternary geology of North America in relation to the migration of man. In: Jenness, D. (Ed.), *The American Aborigines*. University of Toronto Press, Toronto, pp. 11–45.

Kohl, C., Nishiizumi, K., 1992. Chemical isolation of quartz for measurement of in situ-produced cosmogenic nuclides. *Geochimica et Cosmochimica Acta* 6, 3583–3587.

Lal, D., 1991. Cosmic ray labeling of erosion surfaces: in situ nuclide production rates and erosion models. *Earth and Planetary Science Letters* 104, 424–439.

Lambeck, K., Purcell, A., Zhao, S., 2017. The North American late Wisconsin ice sheet and mantle viscosity from glacial rebound analyses. *Quaternary Science Reviews* 158, 172–210.

Mandryk, C.A.S., Josenhans, H., Fedje, D.W., Mathewes, R.W., 2001. Late Quaternary paleoenvironments of Northwestern North America: implications for inland versus coastal migration routes. *Quaternary Science Reviews* 20, 301–314.

Margold, M., Jansson, K.N., Kleman, J., Stroeven, A.P., Clague, J.J., 2013. Retreat pattern of the Cordilleran Ice Sheet in central British Columbia at the end of the last glaciation reconstructed from glacial meltwater landforms. *Boreas* 42, 830–847.

Margold, M., Stokes, C.R., Clark, C.D., 2015. Ice streams in the Laurentide Ice Sheet: identification, characteristics and comparison to modern ice sheets. *Earth-Science Reviews* 143, 117–146.

Margold, M., Stokes, C.R., Clark, C.D., 2018. Reconciling records of ice streaming and ice margin retreat to produce a palaeogeographic reconstruction of the deglaciation of the Laurentide Ice Sheet. *Quaternary Science Reviews* 189, 1–30.

Margold, M., Stroeven, A.P., Clague, J.J., Heyman, J., 2014. Timing of terminal Pleistocene deglaciation at high elevations in southern and central British Columbia constrained by ^{10}Be exposure dating. *Quaternary Science Reviews* 99, 193–202.

McCallum, K.J., Wittenberg, J., 1968. University of Saskatchewan Radiocarbon Dates V. *Radiocarbon*, 10, 365–378.

Menounos, B., Goehring, B.M., Osborn, G., Margold, M., Ward, B., Bond, J., Clarke, G.K.C., *et al*., 2017. Cordilleran Ice Sheet mass loss preceded climate reversals near the Pleistocene termination. *Science* 358, 781–784.

Mott, R.J., 1973. *Palynological Studies in Central Saskatchewan: Pollen Stratigraphy from Lake Sediment Sequences*. Geological Survey of Canada, Ottawa.

Mountjoy, E.W., 1958. Jasper Area Alberta, a source of the Foothills Erratics Train. *Bulletin of Canadian Petroleum Geology* 6, 218–226.

Munyikwa, K., Feathers, J.K., Rittenour, T.M., Shrimpton, H.K., 2011. Constraining the late Wisconsinan retreat of the Laurentide ice sheet from western Canada using luminescence ages from postglacial aeolian dunes. *Quaternary Geochronology* 6, 407–422.

Munyikwa, K., Rittenour, T.M., Feathers, J.K., 2017. Temporal constraints for the late Wisconsinan deglaciation of western Canada using eolian dune luminescence chronologies from Alberta. *Palaeogeography, Palaeoclimatology, Palaeoecology* 470, 147–165.

Newton, B., 1991. Bow Corridor Project: Summary of the 1988–1989 Research. In: Magne, M. (Ed.), Archaeology in Alberta, 1988 and 1989, pp. 113–125. Archaeological Survey, Provincial Museum of Alberta, Occasional Paper No. 33. Alberta Culture and Multiculturalism, Edmonton, Alberta.

Nishiizumi, K., Imamura, M., Caffee, M.W., Southon, J.R., Finkel, R.C., McAninch, J., 2007. Absolute calibration of ^{10}Be AMS standards. *Nuclear Instruments and Methods in Physics Research* B 259, 403–413.

Pedersen, M.W., Ruter, A., Schweger, C., Friebe, H., Staff, R.A., Kjeldsen, K.K., Mendoza, M.L., *et al*., 2016. Postglacial viability and colonization in North America's ice-free corridor. *Nature* 537, 45–49.

Peltier, W.R., 2004. Global glacial isostasy and the surface of the ice-age Earth: the ICE-5 G (VM2) model and GRACE. *Annual Review of Earth and Planetary Sciences* 32, 111–149.

Peltier, W.R., Argus, D.F., Drummond, R., 2015. Space geodesy constrains ice age terminal deglaciation: the global ICE-6G_C (VM5a) model. *Journal of Geophysical Research: Solid Earth* 120, 2014JB011176.

Phillips, F.M., Argento, D.C., Balco, G., Caffee, M.W., Clem, J., Dunai, T.J., Finkel, R., *et al*., 2016a. The CRONUS-Earth project: a synthesis. *Quaternary Geochronology* 31, 119–154.

Phillips, F.M., Argento, D.C., Bourlès, D.L., Caffee, M.W., Dunai, T.J., Goehring, B., Gosse, J.C., *et al*., 2016b. Where now? Reflections on future directions for cosmogenic nuclide research from the CRONUS projects. *Quaternary Geochronology* 31, 155–159.

Porter, S.C., Swanson, T.W., 1998. Radiocarbon age constraints on rates of advance and retreat of the Puget Lobe of the Cordilleran Ice Sheet during the last glaciation. *Quaternary Research* 50, 205–213.

Potter, B.A., Baichtal, J.F., Beaudoin, A.B., Fehren-Schmitz, L., Haynes, C.V., Holliday, V.T., Holmes, C.E., Ives, J.W., *et al*., 2018a. Current evidence allows multiple models for the peopling of the Americas. *Science Advances* 4, eaat5473.

Potter, B.A., Beaudoin, A.B., Haynes, C.V., Holliday, V.T., Holmes, C.E., Ives, J.W., Kelly, R., *et al*., 2018b. Arrival routes of first Americans uncertain. *Science* 359, 1224–1225.

Potter, B.A., Reuther, J.D., Holliday, V.T., Holmes, C.E., Miller, D.S., Schmuck, N., 2017. Early colonization of Beringia and Northern North America: chronology, routes, and adaptive strategies. *Quaternary International* 444, 36–55.

Praetorius, S.K., Mix, A.C., 2014. Synchronization of North Pacific and Greenland climates preceded abrupt deglacial warming. *Science* 345, 444–448.

Rains, R.B., Shaw, J., Sjogren, D.B., Munro-Stasiuk, M.J., Robert Skoye, K., Young, R.R., Thompson, R.T., 2002. Subglacial tunnel channels, Porcupine Hills, southwest Alberta, Canada. *Quaternary International* 90, 57–65.

Rasmussen, S.O., Bigler, M., Blockley, S.P., Blunier, T., Buchardt, S.L., Clausen, H.B., Cvijanovic, I., *et al*., 2014. A stratigraphic framework for abrupt climatic changes during the last glacial period based on three synchronized Greenland ice-core records: refining and extending the INTIMATE event stratigraphy. *Quaternary Science Reviews* 106, 14–28.

Reimer, P.J., Bard, E., Bayliss, A., Beck, J.W., Blackwell, P.G., Ramsey, C.B., Buck, C.E., *et al*., 2013. IntCal13 and Marine13

radiocarbon age calibration curves 0–50,000 years cal BP. *Radiocarbon* 55, 1869–1887.

Roed, M.A., Mountjoy, E.W., Rutter, N.W., 1967. The Athabasca Valley erratics train and ice movement across the Continental Divide. *Canadian Journal of Earth Sciences* 4, 625–632.

Ross, M., Campbell, J.E., Parent, M., Adams, R.S., 2009. Palaeo-ice streams and the subglacial landscape mosaic of the North American mid-continental prairies. *Boreas* 38, 421–439.

Seguinot, J., Rogozhina, I., Stroeven, A.P., Margold, M., Kleman, J., 2016. Numerical simulations of the Cordilleran ice sheet through the last glacial cycle. *Cryosphere* 10, 639–664.

Shapiro, B., Drummond, A.J., Rambaut, A., Wilson, M.C., Matheus, P.E., Sher, A.V., Pybus, O.G., *et al*., 2004. Rise and fall of the Beringian Steppe bison. *Science* 306, 1561–1565.

Stalker, A.M., 1956. *The Erratics Train Foothills of Alberta*. Geological Survey of Canada, Ottawa.

Stone, J.O., 2000. Air pressure and cosmogenic isotope production. *Journal of Geophysical Research: Solid Earth* 105, 23753–23759.

Stroeven, A.P., Fabel, D., Margold, M., Clague, J.J., Xu, S., 2014. Investigating absolute chronologies of glacial advances in the NW sector of the Cordilleran Ice Sheet with terrestrial in situ cosmogenic nuclides. *Quaternary Science Reviews* 92, 429–443.

Stumpf, A.J., Broster, B.E., Levson, V.M., 2000. Multiphase flow of the late Wisconsinan Cordilleran ice sheet in western Canada. *Geological Society of America Bulletin* 112, 1850–1863.

Tarasov, L., Dyke, A.S., Neal, R.M., Peltier, W.R., 2012. A data-calibrated distribution of deglacial chronologies for the North American ice complex from glaciological modeling. *Earth and Planetary Science Letters* 315, 30–40.

Ullman, D.J., Carlson, A.E., Hostetler, S.W., Clark, P.U., Cuzzone, J., Milne, G.A., Winsor, K., Caffee, M., 2016. Final Laurentide ice-sheet deglaciation and Holocene climate-sea level change. *Quaternary Science Reviews* 152, 49–59.

White, J.M., Mathewes, R.W., Mathews, W.H., 1979. Radiocarbon dates from Boone Lake and their relation to the 'ice-free corridor' in the Peace River District of Alberta, Canada. *Canadian Journal of Earth Sciences* 16, 1870–1874.

White, J.M., Mathewes, R.W., Mathews, W.H., 1985. Late Pleistocene chronology and environment of the 'ice-free corridor' of northwestern Alberta. *Quaternary Research* 24, 173–186.

Wolfe, S., Huntley, D., Ollerhead, J., 2004. Relict late Wisconsinan dune fields of the northern Great Plains, Canada. *Géographie physique et Quaternaire* 58, 323–336.

Young, R.R., Burns, J.A., Smith, D.G., Arnold, L.D., Rains, R.B., 1994. A single, late Wisconsin, Laurentide glaciation, Edmonton area and southwestern Alberta. *Geology* 22, 683–686.

Zweck, C., Zreda, M., Desilets, D., 2013. Snow shielding factors for cosmogenic nuclide dating inferred from Monte Carlo neutron transport simulations. *Earth and Planetary Science Letters* 379, 64–71.